FATIGUE LIFETIME OF A SILICA FILLED RUBBER. APPLICATION TO A SBR SHOE SOLE UNDER BENDING.

A. Robisson [1, 2], F. Laraba-Abbès [1], L. Laïarinandrasana [1], R. Piques [1], J.L. Chaverot [2]

[1] Centre des Matériaux P.M. Fourt, Ecole des Mines de Paris, UMR CNRS 7633
BP 87, 91003 Evry Cedex, France
[2] Centre Technique du Cuir, de la Chaussure et de la Maroquinerie, Lyon, France

ABSTRACT

This paper is devoted to the fatigue behaviour characterization of a silica filled styrene butadiene rubber (SBR). The first part concerns the experimental mechanical behaviour characterization of the material. Mechanical tests performed on both pure and filled gum highlight the large influence of the silica fillers on both damage and viscoelasticity of the compound. The identification of the visco-hyperelastic-damage-induced constitutive law parameters is based on uniaxial tests (tension and compression) under static, cyclic and relaxation loadings. The validation of the constitutive equation is performed by finite element analysis computations on axisymmetrically notched specimens, used for fatigue tests. Numerical results show a good agreement with experiments. Local strains and stresses are then calculated to evaluate the material fatigue lifetime. In the second part, the fatigue behavior is investigated. We aim to establish a fatigue crack initiation criterion, from the analysis of uniaxial and torsion tests performed on axisymmetrically notched specimens. Two parameters have an influence on the fatigue lifetime : the maximum of the largest principal strain, and the second strain-amplitude invariant. SEM fracture surface observations highlight the mechanisms of the crack initiation. Fracture takes place from points of weakness like silica filler heterogeneities or molding defects. A multiaxial crack initiation criterion is finally proposed for the prediction of the crack initiation number of cycles for a multiaxially loaded structure.

INTRODUCTION

Shoe soles are generally made of thermoplastic elastomers (PolyChloride of Vinyle (PVC), Ethylene - Vinyle Acetate (EVA)) or thermosets. Among the latters, one can mention Natural Rubber (NR), Butadiene Styrene Rubber (SBR), Polychloroprene Rubber (CR) or Butadiene-AcroNitrile Rubber (NBR). Shoe soles experience large strains (several tens of percents). They also undergo creep under compressive loadings, crack initiation and growth under bending and abrasive wear under frictional forces. This work is devoted to the determination of a fatigue crack initiation criterion of a silica filled styrene butadiene rubber. This material is widely used in the industry of city shoe soles and sport footwear. This paper is split up into two parts : the first one describes the methodology adopted for the identification and the validation of the visco-hyperelastic-damage-induced constitutive equation. Thereby, this step allows us to evaluate the local strains and stresses by a finite element analysis. In the second part of this work, we discuss the influence of some mechanical parameters on the fatigue behavior, more particularly the amplitude and the maximum of the largest principal strain in case of an uniaxial loading. The extension to a multiaxial loading state involves the retention of the second strain-amplitude invariant, associated with the largest principal strain.

Furthermore, SEM fracture surface observations highlight the fatigue failure stress-raisers, especially silica filler heterogeneities and molding defects, from which a crack initiates. Finally, the correlation between the strain state and the crack initiation number of cycles allows us to establish a criterion for the fatigue lifetime prediction.

PART I : IDENTIFICATION OF THE CONSTITUTIVE EQUATION

The Styrene Butadiene Rubber : Compound Formulation and Microstructure

The material under study is a silica filled Styrene Butadiene Rubber (SBR). A Scanning Electron Microscopy observation of a microtomed slice is given in *Figure 1*. The microstructure appears to be strongly filled with silica aggregates (1 to 5 μm) and silica agglomerates (10 to 50 μm). A chemical analysis gives a silica filler concentration of about 33 % (percentage in weight). Furthermore, Wave Dispersive Spectrometry (WDS) local analysis indicates that these fillers are in fact silica-particles-occluded-gum clusters. Notice that silica is added to the compound formulation to improve abrasion properties of the material.

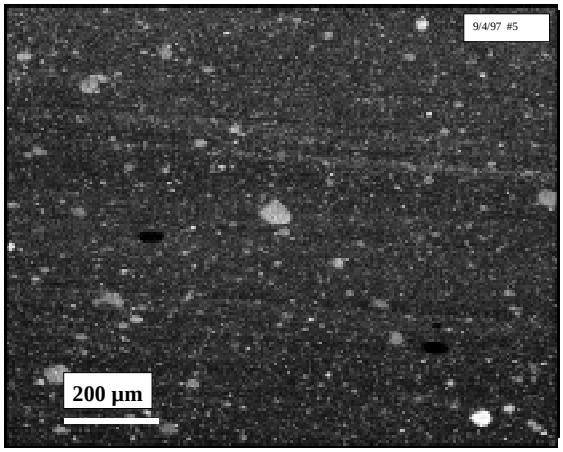

Figure 1: Silica Filled SBR Microstructure

Experimental Procedures and Results

The mechanical behavior characterization is based on uniaxial traction and compression tests under static, cyclic and relaxation loadings. These tests have been performed on both filled and pure gum, to highlight the influence of the silica fillers on the damage and the viscohyperelastic behaviour of the material. The uniaxial tensile test specimens are rectangular strips of 20*150 mm^2, cut off from calandred sheets of 3 mm thickness. As for the uniaxial compression tests, they have been performed on axisymmetric samples cut off from injected blocks.

Uniaxial traction (UT) and compression (UC) tests

The experimental results of *Figure 2* are given in terms of the evolution of the nominal stress (1^{st} Piola-Kirchhoff stress) $K_1 = F/S_0$ versus the stretch ratio $\lambda_1 = L/L_0$. "F" denotes here the actual load, "S_0" the initial cross section area, "L" the actual length of the specimen and "L_0" its initial value. One can notice the nonlinear behavior of the material, and the large extension level achieved (up to 400% of nominal strain). The initial UT tangent modulus of the silica filled SBR is about 100 MPa. By contrast, the pure gum one is about 5 MPa. At larger stretch ratios, the tangent modulus values for filled and unfilled materials are quasi similar. Such observations suggest that the very strong value of the initial tangent modulus is due to the filler reinforcement. Furthermore, this effect is annihilated by the silica filler network disruption [1].

Relaxation tests under traction and compression loadings

Typical experimental results of relaxation tests performed under tensile and compression loadings are given in *Figure 3*. Both filled and unfilled gum have been tested. The imposed final extensions have been reached in 0.2 s for the uniaxial traction tests, and in 0.5 s for the uniaxial compression ones. The experimental nominal stresses have been normalized by the corresponding maximal nominal stress value (K_{1max}) reached just after the loading step. In the range of the extension levels investigated here, one can notice the quasi similar rate of decrease of the nominal stress for the silica filled rubber under tension and compression loadings. This observation suggests the same relaxation kinetics. Moreover, the filled-gum-stress-relaxation rate is higher than the pure-gum one. This result highlights the influence of the fillers on the viscoelastic component of the material behavior.

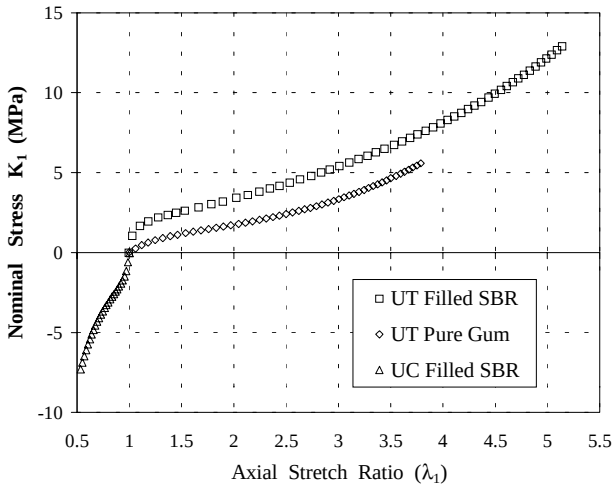

Figure 2: Uniaxial Traction and Compression Tests on SBR (Strain Rate $\dot{\varepsilon}$=0.015 s^{-1}).

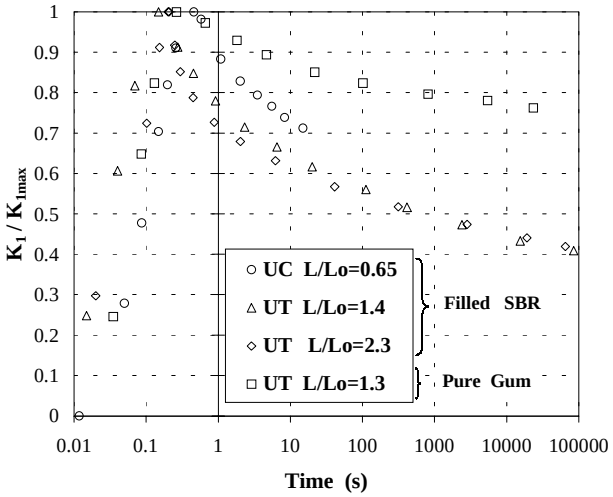

Figure 3: Uniaxial Traction and Compression Relaxation Tests on SBR.

Cyclic behaviour under tensile loading conditions

Figure 4 illustrates the tensile cyclic behaviour of the silica filled rubber. The loading step has been performed with an imposed displacement, and the unloading sequence is stress-controlled, with the nominal stress minimum value set to zero to avoid any specimen buckling. The cyclic loading response of the material exhibits a large hysteresis, essentially during the first cycle. We can also notice the non negligible permanent set, in addition to the progressive creep. Moreover, the latter increases with the imposed final extension, whereas the secant modulus decreases. In addition, the comparison of the cyclic behavior between the filled rubber and the pure gum illustrates the strong influence of the fillers on the dissipation rate and the permanent set (see *Figure 5*).

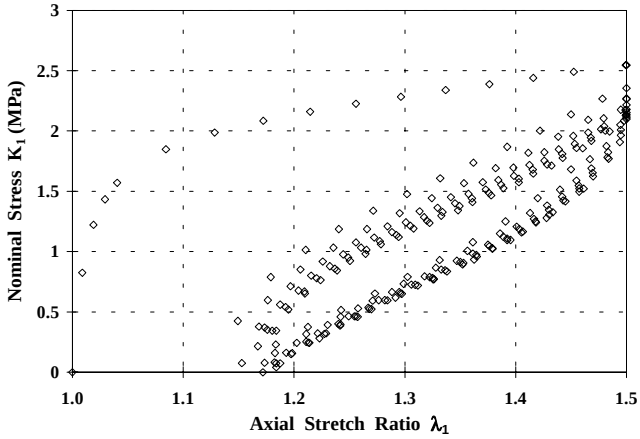

Figure 4: Cyclic Behaviour of the Silica Filled SBR (Strain Rate $\dot{\varepsilon}$=0.01 s^{-1}).

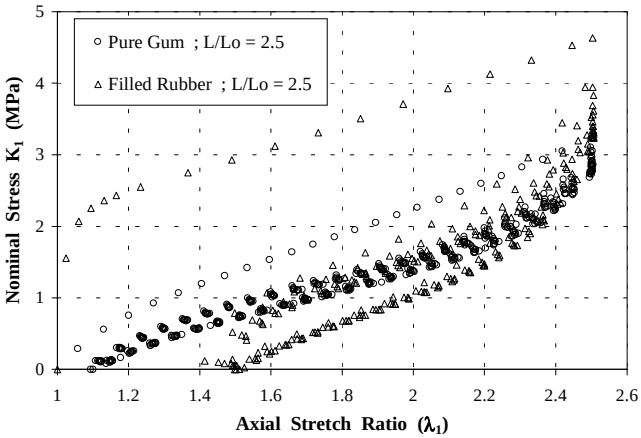

Figure 5: Cyclic Behaviour of both Pure Gum and Silica Filled SBR

Permanent or recoverable effects ?

A question remains open : do fillers damage the material, or are all the described phenomena (permanent set, viscoelasticity, stress-softening) recoverable? The main difficulty is to split up the viscoelastic effects from the damage ones. A silica filled SBR sample has been stretched to a fixed extension. After a 48 hours-release, we stretched it again. It is supposed throughout that the viscoelastic properties are mostly recovered during this time.

Experimental results show that the stress-softening induces a permanent loss of strength. Unless a temperature restoration, this phenomenon is then similar to damage. Moreover, we also checked that the damage process is not isotropic.

Modeling the Behavior of the Silica Filled SBR

The visco-hyperelastic-damage-induced constitutive equation

The general framework of this study is the finite transformations. Assuming incompressibility, homogeneity and isotropy, the hyperelastic stress-strain relationship is derived from the Rivlin's strain energy function "W". The expansion at the second order-deformation and the retention of three parameters leads to Eqn. 1.:

$$W(I_1, I_2) = c_{10}(I_1 - 3) + c_{01}(I_2 - 3) + c_{20}(I_1 - 3)^2 \tag{1}$$

where I_1 and I_2 refer to the first and the second right-Cauchy-Green dilatation tensor invariants, respectively, and c_{ij} are the constitutive law parameters. Johnson and al. [2] suggest to constrain the c_{ij} parameters to satisfy the Drucker postulate of stability $d\mathbf{T}.d\mathbf{A} \geq 0$, where $\mathbf{T}$ denotes the Cauchy stress tensor, and $\mathbf{A}$ the Almansi-Euler strain tensor. This condition leads to $c_{ij} \geq 0$.

The viscoelasticity component is modeled using the hereditary integral formulation. The latter is an extension of the small strain linear viscoelasticity theory, given by :

$$\mathbf{T}(t) = \int_0^t [G(t-t') + K(t-t')] \frac{\partial}{\partial t'} \mathbf{A}(t') dt' \tag{2}$$

where G(t) is the shear relaxation modulus and K(t) the bulk relaxation modulus. In order to model the incompressible multiaxial viscoelasticity, we consider only the deviatoric part of the Cauchy stress tensor $\mathbf{T}$. The next step consists in extending the hereditary formulation to the finite strain framework. Notice that although the Boltzmann superposition principle (used to obtain a continuous strain history) is not rigorously valid in case of finite nonlinear elasticity, we will nevertheless use it, as many other authors [2] [3] [4]. In practice, the extension to finite strains is performed by transporting the mechanical entities to the configuration $C^{t-t'}$, instead of the actual configuration C^t, using the transformation gradient tensor $\mathbf{F}$:

$$\mathbf{T}^t(t-t') = \mathbf{F}^{-1t}(t-t')\, \mathbf{T}^{t-t'}(t-t')\, \mathbf{F}^t(t-t') \tag{3}$$

Moreover, the monotonically decreasing shear relaxation modulus G(t) is approximated by a Prony series (discrete spectrum of relaxation times) :

$$G(t) = G_0 + \sum_i g_i \, e^{(-t/\tau_i)} \tag{4}$$

where g_i and τ_i refer to the relaxation strengths and the retardation times, respectively. According to the experimental results, we impose one relaxation time per decade : $\tau_1 = 0.2$ s, $\tau_2 = 2$ s, $\tau_3 = 20$ s, $\tau_4 = 200$ s, $\tau_5 = 2000$ s. In addition, because of the monotonically decrease of the stress during the relaxation tests, we impose the following constraint : $g_1 > g_2 > g_3 > g_4 > g_5$.

As for the stress-softening effect, the experimental results show that damage occurs mostly during the first stretching of the sample : damage is then discontinuous. According to these observations, we consider a multiaxial discontinuous damage evolution, which takes into account the maximum principal strain gradient component $\mathbf{F}_1$ previously reached during the material history of load. The equation is close to Miehe's model [5], and the damage kinetics is given by Eqn. 5. :

$$\begin{aligned} &\text{If } \dot{\mathbf{F}}_1 > 0 && d(\mathbf{F}_1) = d_\infty \left[1 - \exp\left(-\frac{|F_1 - 1|}{\eta} \right) \right] \\ &\text{If } \dot{\mathbf{F}}_1 = 0 && d(\mathbf{F}_1) = 0 \end{aligned} \tag{5}$$

where d_∞ is the maximal possible damage ($0 \leq d_\infty \leq 1$) and η is a parameter characteristics of the range of extension in which damage occurs.

Identification of the constitutive equation parameters

The major difficulty is inherent to the number of parameters to be identified, that is 10 parameters.The evolutionary algorithm is used as an optimization method, implemented into the finite element code ZeBuLoN of the Centre des Matériaux. The successive steps of the optimization procedure are summarized as follows :

1) First determination of the hyperelastic parameters c_{ij} and the damage parameters (d_∞ , η) from the monotonic uniaxial traction and compression tests, at a strain rate $\dot{\varepsilon}$=3 s^{-1}.
2) Determination of the relaxation strengths g_i from the uniaxial tensile relaxation tests.
3) Final identification of the c_{ij} parameters from the cyclic uniaxial traction and compression tests.

Finally, the optimized parameters are given below (see *Table 1*) :

TABLE 1
THE CONSTITUTIVE EQUATION PARAMETERS

c_{10} (MPa)	c_{01} (MPa)	c_{20} (MPa)	d_∞	η
2.668	0.271	0.466	0.914	0.719

τ_1 (s)	g_1	τ_2 (s)	g_2	τ_3 (s)	g_3	τ_4 (s)	g_4	τ_5 (s)	g_5
0.2	0.3015	2.0	0.1218	20	0.0876	200	0.0783	2000	0.0461

Figure 6 and *Figure 7* show the good agreement between the experimental data and the numerical results issued from the identification of the constitutive law parameters, for a strain rate value of 0.01 s^{-1} and 0.1 s^{-1}, respectively. It is worth noting that the model underestimates the hysteresis dissipation. Such results are probably related to the integral formulation of the viscoelasticity. An alternative formulation, based on a thermodynamics approach, has been proposed elsewhere [6].

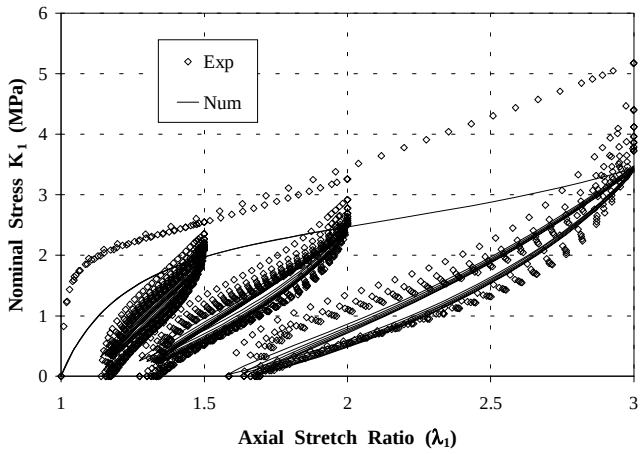

Figure 6: Cyclic Behaviour of the Silica Filled SBR (Strain Rate $\dot{\varepsilon}$=0.01 s^{-1}).

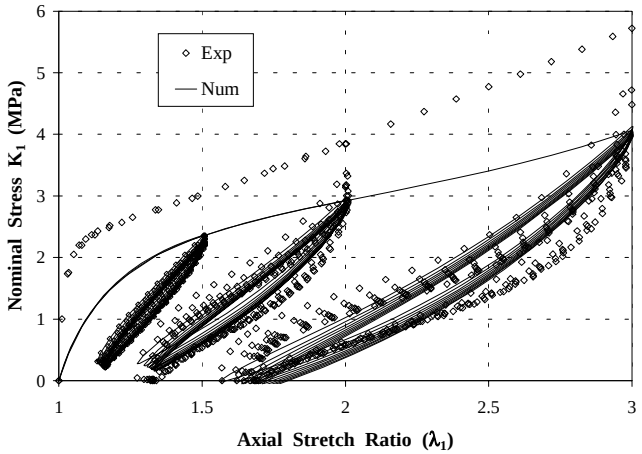

Figure 7: Cyclic Behaviour of the Silica Filled SBR (Strain Rate $\dot{\varepsilon}$=0.1 s^{-1}).

Validation of the constitutive equation

The validation of the constitutive law has been performed by the comparison between the experimental data issued from both tension-compression and torsion tests carried on axisymmetric notched specimens, and the numerical results issued from finite element computations. *Figure 8* and *Figure 9* illustrate the good agreement between the experimental data and the numerical results. Notice that both tension-compression and torsion frequency load is about 0.3 Hz, compared to 0.1 Hz and 0.01 Hz for the previous mechanical tests. Moreover, the simulated load and torque of the first loading do not fit the experimental data. However, the first cycle is not considered in the fatigue study, because of its transient nature. On the other hand, numerical results are in a good agreement with the experimental data on the stabilized cycles, even though the multiaxial state of the deformation.

These observations validate the constitutive equation, and local strains and stresses are then computed for the fatigue lifetime prediction, described below.

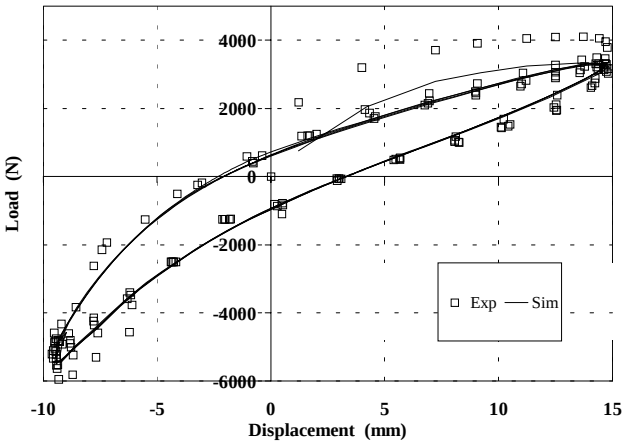

Figure 8: Tension-Compression Test on an Axisymmetric Notched Specimen (-10 _ 15 mm).

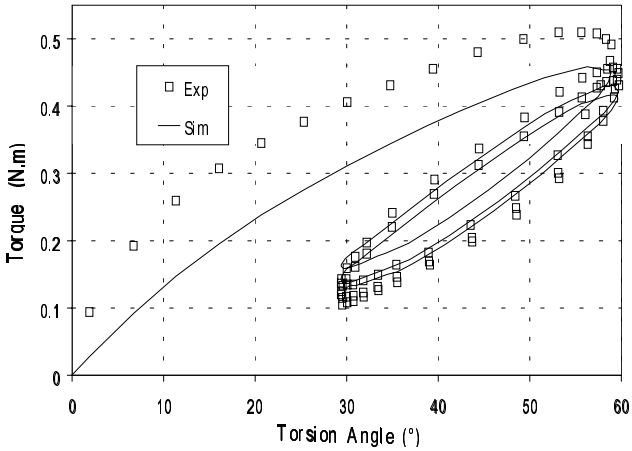

Figure 9: Torsion Test on an Axisymmetric Notched Specimen (30° _ 60°).

PART II : FATIGUE BEHAVIOUR AND LIFETIME PREDICTION

This section concerns the investigation of the silica filled fatigue behaviour, especially the fatigue crack initiation mechanisms and the fatigue lifetime prediction.

Determination of the Pertinent Mechanical Parameters for the Description of the Fatigue Behaviour

Tension-compression and torsion tests have been performed on axisymmetric notched specimens. The root notch is about 40 mm in the first case (NS1), and 2 mm in the second one (NS2). The crack initiation is macroscopically detected from a critical size of 1 mm.

The following curves illustrate the evolution of the two parameters that influence the fatigue lifetime of the material in case of a multiaxial loading : the maximum of the largest principal strain E_{pmax} (*Figure 10*), and the second strain-amplitude invariant ΔE_{II} (*Figure 11*). "N_i" denotes here the number of crack initiation cycles.

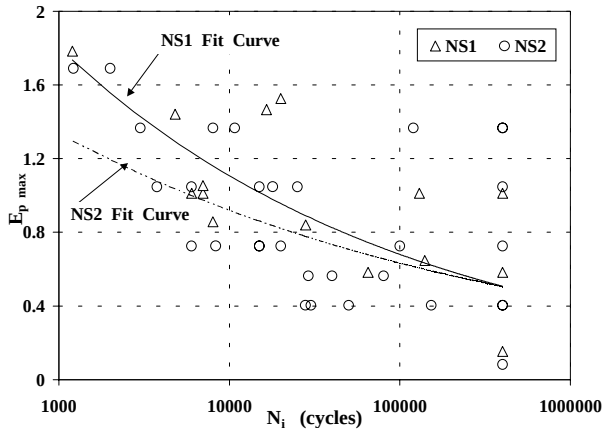

Figure 10: Evolution of the Maximum of the Largest Principal Strain.

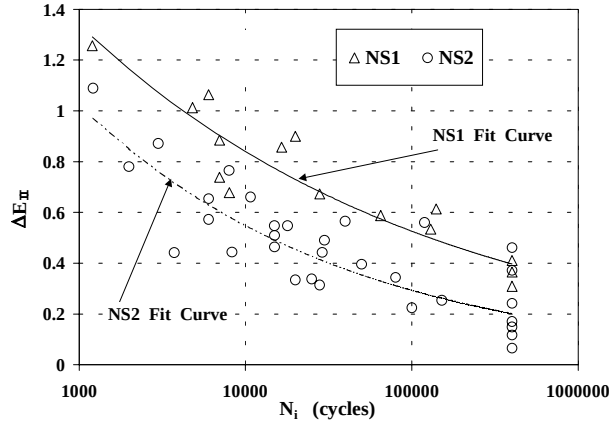

Figure 11: Evolution of the Amplitude of the Largest Principal Strain.

The Crack Initiation Stress-Raisers

SEM observations performed on both "static" and "cyclic" samples allowed us to evidence the crack initiation points of weakness. In the first case, fracture takes place from three principal sites, according to the

extension level achieved. At small extensions ($\lambda_1 \approx 1.1$), silica-filler-occluded-gum clusters exhibit a "S" disruption (*Figure 12*). Increasing the stretch ratio level induces the two-parts complete rupture of the cluster

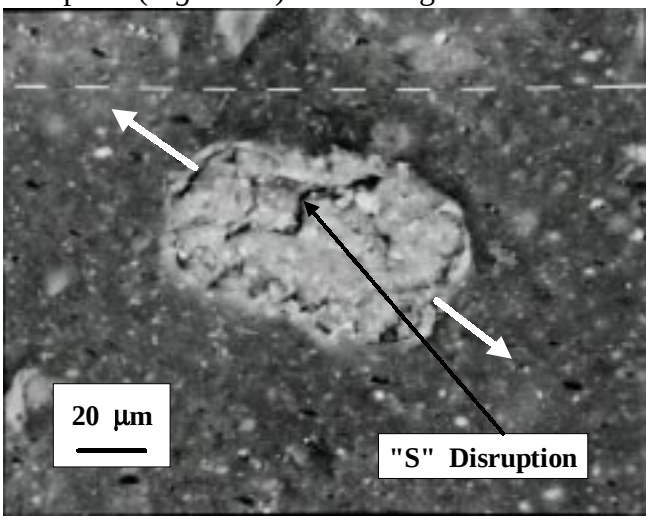

Figure 12: Silica Agglomerate "S" Disruption (SEM in-situ tensile test, $\lambda_1 = 1.1$)

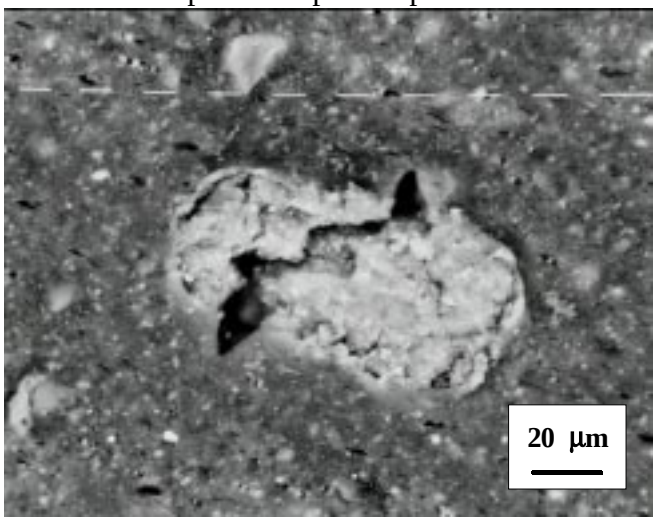

Figure 13: Complete Disruption of the Silica Cluster and Extension to the Gum ($\lambda_1 = 1.5$).

Figure 14: Large extension of an Inter-Aggregates Gum Ligament.

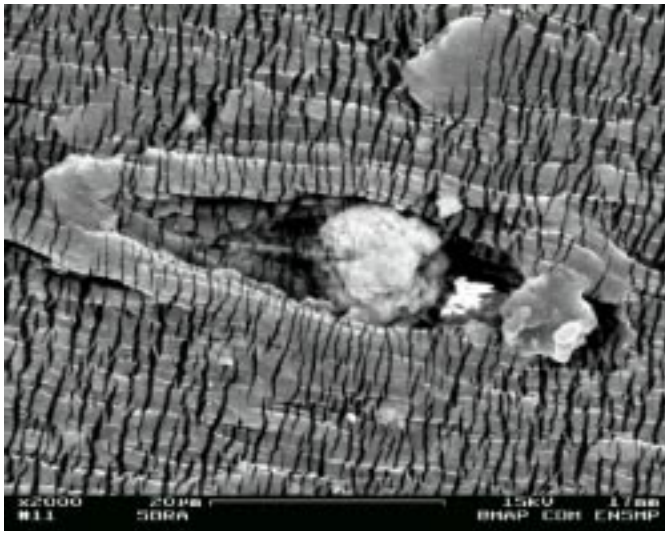

Figure 15: Decohesion of a Silica Filler Aggregate.

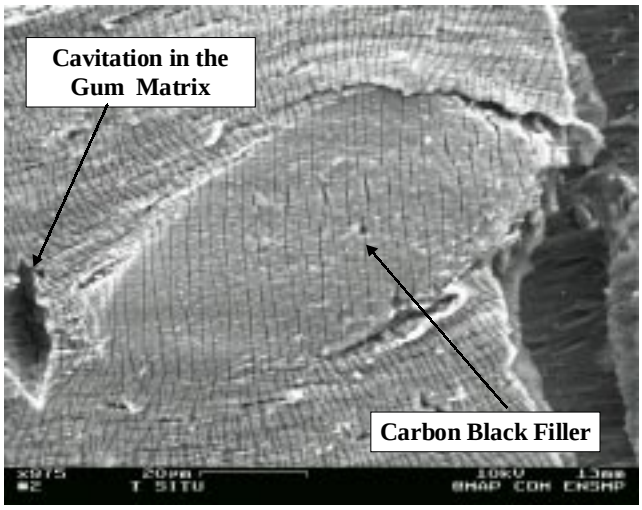

Figure 16: Cavitation in the Gum Matrix, close to a Carbon Black Agglomerate, $\lambda_1 = 3$.

(*Figure 13*). A zoom of this cluster shows the large extension of the inter-aggregates gum ligament, to accomodate the macroscopic strain (*Figure 14*). Furthermore, decohesion of silica aggregates is also observed (*Figure 15*). Finally, at higher stretch ratios ($\lambda_1 \approx 3$), cavitation takes place in the gum matrix, close to carbon black agglomerates (*Figure 16*).

As for the "cyclic" samples, SEM observations evidenced that fracture also initiates on silica heterogeneities, even at low extensions. The fracture surface generally exhibits a "bean" morphology (*Figure 17*, *Figure 19*). Some silica segregations or gum-kaolin clusters are evidenced in the middle zone of the samples (*Figure 18*, *Figure 20*). The diversity of these stress-raisers finally justify the previously noticed experimental scatter on the crack initiation number of cycles (*Figure 10* and *Figure 11*).

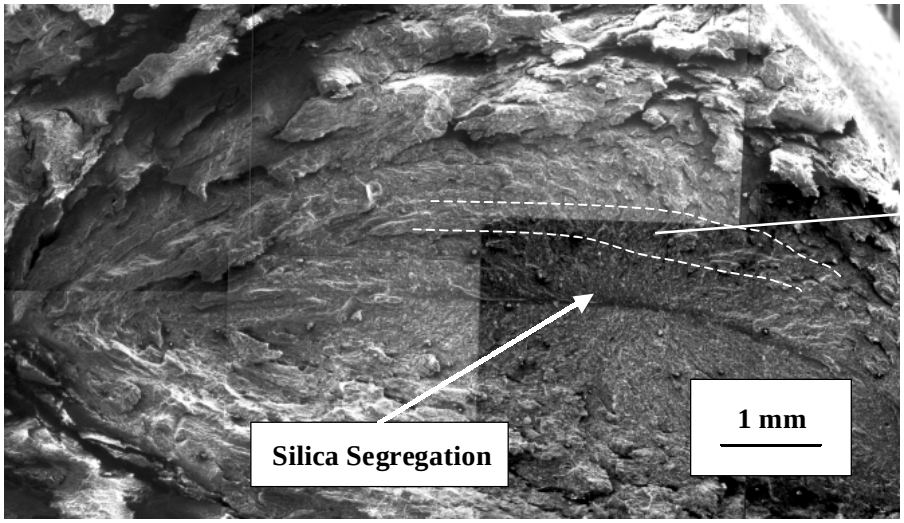

Figure 17: "Bean" Morphology of the Fracture Surface.

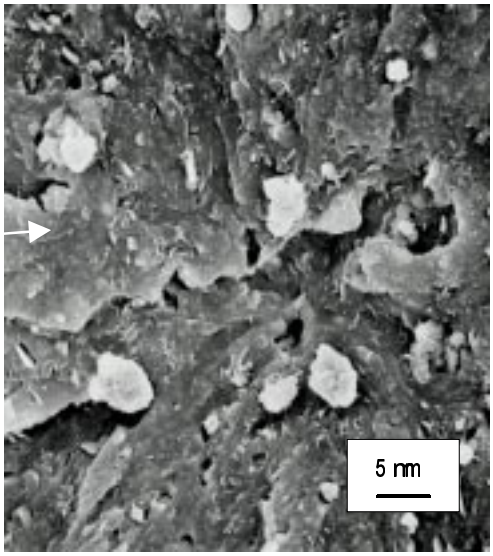

Figure 18: Kaolin-Gum Clusters.

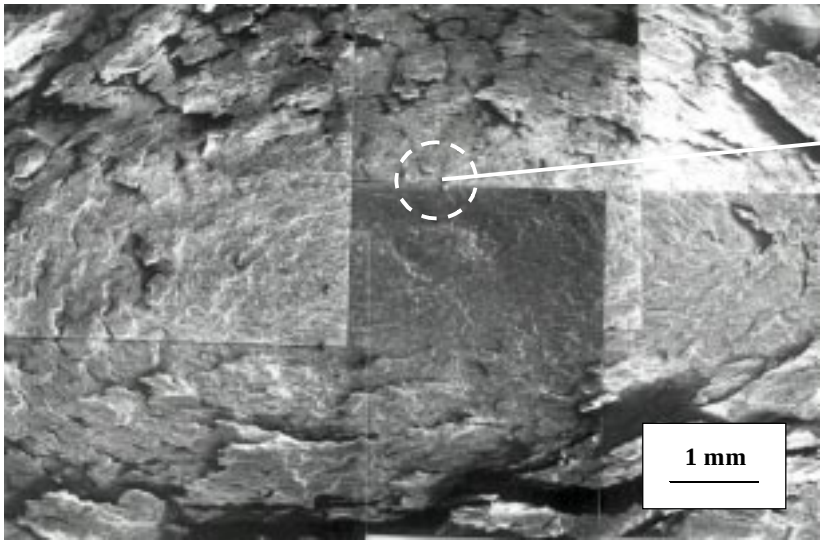

Figure 19: Another "Bean" Morphology of the Fracture Surface.

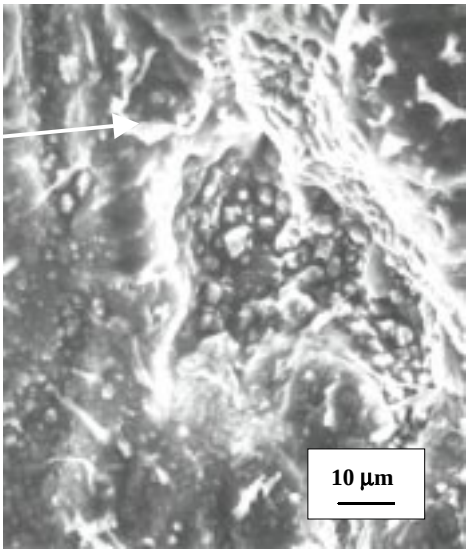

Figure 20: Silica Agglomerate.

The Fatigue Lifetime Prediction Criterion

The correlation between the strain state and the crack initiation number of cycles allowed us to establish a fatigue lifetime prediction criterion. Its expression is given below :

$$N_i = 9\,500 \,.\, \exp\left[\frac{-\Delta E_{II} + 0.321 E_{p\,max}{}^2 - 0.341 E_{p\,max} + 0.566}{0.112}\right] \qquad (6)$$

This criterion has been successively applied to the lifetime prediction of shoe soles (see [6]).

ACKNOWLEDGEMENTS

Authors would like to thank the CTC for its industrial support and collaboration for this study.

REFERENCES

1. Wolff, S. (1996). *Rubber Chemistry and Technology*. **69**(3), 325.
2. Johnson, A.R., Quigley, C.J.and Mead, J.L. (1994). *Rubber Chemistry and Technology*. **67**(5), 904.
3. Bernstein, B., Kearsley, E.A. and Zapas, L.J. (1963). *Transactions of the Society of Rheology*. **7**, 391.
4. Tanner, R.I. (1988). *Journal of Rheology*. **32**(7), 673.

5. Miehe, C. (1995). *Journal of Mechanics*. **14**(5), 697.
6. Robisson, A. (2000). *PhD Thesis (Ecole des Mines de Paris)*, to be published.